PHYSICAL REVIEW D **88,** 076003 (2013)

Kaluza-Klein gluon searches using the three-b-jet decay channel at the Large Hadron Collider

Masato Arai,[1,3,*] Gi-Chol Cho,[2,†] and Karel Smolek[3,‡]

[1]*Fukushima National College of Technology, Fukushima 970-8034, Japan*
[2]*Department of Physics, Ochanomizu University, Tokyo 112-8610, Japan*
[3]*Institute of Experimental and Applied Physics, Czech Technical University in Prague, Horská 3a/22, 128 00 Prague 2, Czech Republic*

(Received 1 August 2013; published 2 October 2013)

We study observability of a Kaluza-Klein (KK) excitation of a gluon in a five-dimensional model with a warped geometry at the Large Hadron Collider. In this model, the Standard Model fields reside in the bulk and the third generation quarks couple to the KK gluon strongly. We focus on the processes including three b quarks as a final state where the first KK gluon propagates as an intermediate state. We evaluate a significance of those processes by taking account of kinematical cuts and a detector efficiency at the Large Hadron Collider and find that the significance is lager than 5σ with the integrated luminosity of 10 (100) fb^{-1} for a certain range of parameters of the model.

DOI: 10.1103/PhysRevD.88.076003 PACS numbers: 11.10.Kk, 12.60.−i

I. INTRODUCTION

A possibility that our world is embedded into a higher dimensional space-time has been intensively studied. A strong motivation to study such a model is to solve the hierarchy problem between the electroweak scale and the Planck scale. The warped extra-dimensional model proposed by Randall and Sundrum (RS) [1] is one of the promising candidates to explain such a large hierarchy. This is a five-dimensional model where one extra-dimension is compactified on the orbifold $S^1/\mathbf{Z}_2$. There are two 3-branes located at different positions on this orbifold with opposite brane tensions. One of the branes is called the visible brane where the Standard Model (SM) fields localize and the other is called the hidden brane. Only a graviton can propagate into the whole space-time. With this setup, it is shown that an effective mass scale on the visible brane can be the electroweak scale as a consequence of the warped geometry, which is a natural solution of the hierarchy problem.

Although in the original RS model all the SM fields localize on the brane, in order to solve the hierarchy problem, it is sufficient to localize only the Higgs fields on the visible brane. It has allowed the other SM fields to propagate into the bulk together with the graviton. We call this model the bulk RS model. Phenomenological aspects of this model have been investigated (for instance, see [2,3]). A generic feature of the bulk RS model is that Kaluza-Klein (KK) excitations of the SM fields appear since the fermions and the gauge fields propagate into the bulk. They are signals of new physics if it is observed. In particular, at the Large Hadron Collider (LHC), one of these promising signals is the KK excitations of the gluon since colored particles are dominantly produced at the LHC.

The KK masses of the gluons are, however, severely constrained by tree-level flavor changing neutral currents (FCNCs). Processes mediated by the KK excitations of the gluons can yield effects of large FCNCs, which are constrained by low energy measurements of neutral mesons such as the $K^0 - \bar{K}^0$ mixing. Contributions of KK gauge bosons to a CP violating parameter ϵ_K in that process constrain the KK gauge boson mass to be $M_{\mathrm{KK}} > 20$ TeV. However, it should be noted that these masses can be lowered by choosing the bulk masses of fermions appropriately or assuming some flavor structures of the quark and lepton sectors (for a convenient summary of this issue, see [4]).

Another constraint comes from the electroweak precision tests because of the large contributions of the KK gauge bosons to the oblique parameters. For instance, considering the model that only the gauge bosons propagate into the bulk while the fermions are on the visible brane, the bound of the KK masses is 25–30 TeV [2]. It corresponds to the typical scale of the RS model $\Lambda_\pi \sim 100$ TeV, which leads to the undesirable little hierarchy between the electroweak scale and the lightest nonzero KK mass. It is, however, possible to lower the KK masses to be $\mathcal{O}$ (TeV) by introducing the custodial symmetry [5] or by placing the SM fermions in the bulk [6]. Even it is shown that models without the custodial symmetry make possible the KK gauge boson mass lower to $\mathcal{O}$ (TeV). As is seen above, the bound for the KK gauge boson mass is model dependent and therefore it is worth examining observability of the KK gauge boson mass with a few TeV at the LHC.

The KK gluon search in the bulk RS model has been studied in the processes including top quarks as a final state. For instance, in Refs. [4,7–9], the $t\bar{t}$ final state from the decay of $g^{(1)}_{\mathrm{KK}} \to t\bar{t}$ has been used as a probe of the KK

*masato.arai@fukushima-nct.ac.jp
†cho.gichol@ocha.ac.jp
‡karel.smolek@utef.cvut.cz

gluon, where $g^{(1)}_{\rm KK}$ is the first KK excitation of a gluon. The associated production of $g^{(1)}_{\rm KK}$ decaying to $t\bar{t}$ has been studied in Ref. [10]. Experimental bounds have been obtained by using the decay channel $g^{(1)}_{\rm KK} \to t\bar{t}$. The experimental lower bound on the mass of $g^{(1)}_{\rm KK}$ is of order 1 TeV in both the Tevatron [11] and the LHC [12,13].

The purpose of our work is to study a sensitivity of the first KK excitation of a gluon in the bulk RS model at the LHC by using the b quark final state only, in particular, the process $pp \to 3b$. In our previous paper [14], we studied a sensitivity to observe the KK gluon at the LHC through the decay channel $g^{(1)}_{\rm KK} \to b\bar{b}$ for various choices of couplings of the KK gluons to the SM quarks. We found that the KK gluon with the mass up to 1.4 TeV would be observable with a significance 5σ in the choice of parameters for integrated luminosity of 100 fb^{-1}. In this paper, we consider the case that the KK gluon strongly couples to the right-handed top quark t_R since it is naively expected that such an interaction does not affect electroweak and flavor processes [4,7,8,15]. In addition, we choose the couplings of the KK gluon to the right-handed bottom quark to be as large as the coupling of the KK gluon to the t_R and to be smaller than it. In the literature, it is chosen to be negligibly suppressed since it contributes to FCNC. However, there are various variants of the Yukawa sector in the bulk RS model (e.g., Ref. [9]). Therefore, we leave the coupling of the KK gluon to the left- and right-handed b quark as phenomenological parameters. Detailed choices will be found in the main body.

The organization of this paper is as follows. In Sec. II, we briefly review the bulk RS model with the SM bulk fermions and the gauge bosons. Numerical results are shown in Sec. III. Section IV is devoted to the summary.

II. MODEL

In this section, we briefly review the bulk RS model, focusing on the interactions of the KK gluon (we follow the notation of Ref. [16]). The RS model is a five-dimensional model with a warped fifth dimension. The space-time metric is given by

$$ds^2 = G_{MN}dx^M dx^N = e^{-2\sigma}\eta_{\mu\nu}dx^\mu dx^\nu + dy^2, \quad (2.1)$$

where $\eta_{\mu\nu} = \mathrm{diag}(-1, +1, +1, +1)$ is the Minkowski metric and $\sigma = k|y|$. Throughout this paper, the roman index runs from 0 to 4 while the greek index runs from 0 to 3. The curvature of the AdS_5 is determined by a dimensionful parameter k. Two 3-branes are located at the fixed points of the orbifold $S^1/\mathbf{Z}_2$ with a radius r_c at $y = 0$ and πr_c, which are called the hidden brane and the visible brane, respectively. With this setup, the effective mass scale at the visible brane is given as $M_P e^{-k\pi r_c}$, where M_P is the four-dimensional Planck scale. The effective mass reproduces the electroweak scale when $kr_c \simeq 12$ so that the hierarchy between the electroweak scale and the Planck scale is stabilized without introducing a serious fine-tuning. In the following, we assume that only the SM Higgs field localizes in the visible brane while the other fields propagate into the five-dimensional bulk.

The gauge invariant action of a gauge field A^a_M and a fermion Ψ is given by

$$S_5 = -\int d^4x \int dy \sqrt{-G}\Big[\frac{1}{4}F^a_{MN}F^{MNa} + i\bar{\Psi}\gamma^M D_M \Psi + im_\Psi \bar{\Psi}\Psi\Big], \quad (2.2)$$

where $G = \det(G_{MN})$, F^a_{MN} denotes the field strength of a gauge field A^a_M, and D_M is a covariant derivative. The index $a = 1, \ldots, \dim(\mathcal{G})$ is a gauge index, where $\dim(\mathcal{G})$ is a dimension of a gauge group $\mathcal{G}$. In the following, we choose the color gauge group $\mathrm{SU}(3)_C$ relevant to dynamics of the gluon. The five-dimensional fermion mass parameter m_Ψ is given as

$$m_\Psi = ck\epsilon(y), \quad (2.3)$$

where c is an arbitrary dimensionless parameter, and $\epsilon(y)$ is $+1$ for $y > 0$ while -1 for $y < 0$ to make the mass term to be $\mathbf{Z}_2$ even.

The KK decomposition of a "gluon" $A^a_M(x, y)$ and $\Psi(x, y)$ is given as[1]

$$\Phi(x^\mu, y) = \frac{1}{\sqrt{2\pi r_c}}\sum_{n=0}^{\infty}\Phi^{(n)}(x^\mu)f_n(y), \quad (2.4)$$

where $\Phi = \{A^a_\mu, \Psi\}$ and $\Phi^{(n)}(x^\mu) = \{A^{a(n)}_\mu(x^\mu), \psi^{(n)}(x^\mu)\}$. The mode functions $f_n(y)$ satisfy the orthonormal condition

$$\frac{1}{2\pi r_c}\int_{-\pi r_c}^{\pi r_c} dy e^{(2-s)\sigma} f_n(y) f_m(y) = \delta_{nm}, \quad (2.5)$$

with $s = 2, 1$ for A^a_μ, Ψ. The explicit form of the function f_n for the zero ($n = 0$) and $n(\neq 0)$ modes are given as follows:

$$f_0 = 1, \quad (2.6)$$

$$f_n = \frac{e^\sigma}{N_n}\Big[J_1\Big(\frac{m_n}{k}e^\sigma\Big) + b_1(m_1)Y_1\Big(\frac{m_n}{k}e^\sigma\Big)\Big], \quad (2.7)$$

where J_1 and Y_1 are the standard Bessel functions of the first and second kind, N_n is a normalization factor, $b_1(m_n)$ is the constant, and m_n is the mass of the nth KK mode.

Substituting (2.4) with (2.6) and (2.7) into (2.2) and integrating the y direction, we find the interactions of the gluon and fermions with an arbitrary KK index n. The four-dimensional $\mathrm{SU}(3)_C$ gauge coupling g_4 is obtained from three gluon interactions in (2.2) by integrating out the mode functions as

[1]We adopt a gauge choice $A_4 = 0$.

$$g_4 = g_5 \int_{-\pi r_c}^{\pi r_c} dy \frac{f_0^3}{(2\pi r_c)^{3/2}} = \frac{g_5}{\sqrt{2\pi r_c}}. \quad (2.8)$$

The condition (2.5) tells us that a KK gluon $g_{\rm KK}^{(n)}(n \neq 0)$ does not couple to a zero-mode gluon pair, i.e., there is no $g_{\rm KK}^{(n)}$-g-g vertex, where $g_{\rm KK}^{(n)}$ and g denote the nth excitations of the KK gluon and the four-dimensional gluon, respectively. It is also easy to see that the couplings of $g_{\rm KK}^{(n)}$-$g_{\rm KK}^{(n)}$-g and $g_{\rm KK}^{(n)}$-$g_{\rm KK}^{(n)}$-g-g vertices are identical to the g-g-g and g-g-g-g vertices, respectively [17]. The effective coupling of the interaction vertex of the nth KK gluon and the zero-mode fermion pair is

$$g^{(n)} = g_4 \frac{1-2c}{e^{(1-2c)\pi k r_c} - 1} \times \frac{k}{N_n}\left[J_1\left(\frac{m_n}{k}e^{\sigma}\right) + b_1(m_n) Y_1\left(\frac{m_n}{k}e^{\sigma}\right)\right]. \quad (2.9)$$

More detailed discussion is given in, for example, Refs. [16,17].

We consider the following scenarios with various values of couplings:

$$\frac{g_{Q_3}^{(1)}}{g_4} = \frac{g_t^{(1)}}{g_4} = \frac{g_b^{(1)}}{g_4} = 4, \qquad \frac{g_{\rm light}^{(1)}}{g_4} = 0, \quad (2.10)$$

$$\frac{g_{Q_3}^{(1)}}{g_4} = 1, \qquad \frac{g_t^{(1)}}{g_4} = \frac{g_b^{(1)}}{g_4} = 4, \qquad \frac{g_{\rm light}^{(1)}}{g_4} = 0, \quad (2.11)$$

$$\frac{g_{Q_3}^{(1)}}{g_4} = 1, \qquad \frac{g_t^{(1)}}{g_4} = 4, \qquad \frac{g_b^{(1)}}{g_4} = 1, \qquad \frac{g_{\rm light}^{(1)}}{g_4} = 0, \quad (2.12)$$

$$\frac{g_{Q_3}^{(1)}}{g_4} = 1, \qquad \frac{g_t^{(1)}}{g_4} = 4, \qquad \frac{g_b^{(1)}}{g_4} = \frac{g_{\rm light}^{(1)}}{g_4} = 0. \quad (2.13)$$

where Q_3 is the third generation of the left-handed quark, t, b are the right-handed top and bottom quarks, and "light" means the quarks of the first two generations. In (2.10), couplings of all the quarks of the third generation to the KK gluon is strong while a coupling between the KK gluon and the light quarks is vanishing. The latter choice is motivated by the constraints coming from the FCNC and the electroweak precision measurement. In (2.11), the KK gluon strongly couples to the right-handed quarks only. The coupling to the left-handed quark is comparable to the QCD coupling g_4. This choice has been studied to analyze a decay of the KK gluon to top and antitop quarks [8].[2] In (2.12), the KK gluon coupling to the right-handed bottom quark is taken to be 1 while the rest of the choice is the same as (2.11). This is motivated by the mass hierarchy between the top quark mass and the bottom quark, which would affect the couplings through (2.9). In (2.13) the difference from (2.12) is to take the KK gluon coupling to the right-handed bottom quark to be zero. This choice comes from the flavor physics and the electroweak precision measurement [4]. With the above choice of parameters, we perform the numerical analysis of the process $pp \overset{g_{\rm KK}^{(1)}}{\longrightarrow} 3b$.

[2]Note that the strong coupling of the right-handed b quark to the KK gluon may give a sizable shift of the Zbb vertex in the 1-loop level. Such an effect is, however, marginal even for $g_b^{(1)}/g_4 = 6$ when the KK gluon mass is larger than 500 GeV [18]. Therefore our choice of the couplings in (2.10) and (2.11) does not affect the Zbb vertex since we take $M_{g_{\rm KK}^{(1)}} \geq 1$ TeV in our study.

III. NUMERICAL ANALYSIS

We study effects of the KK gluon predicted by the presented model in the three b final states ($bb\bar{b}$ and $b\bar{b}\,\bar{b}$) at the LHC. Four representative Feynman diagrams describing the studied processes in the leading order are visualized in Fig. 1. The rest of the diagrams can be obtained by using one or more transformations from the following list: the interchanging of b and $\bar{b}$ in a whole diagram, changing the order of the initial partons, and changing the order of the final partons. The presented diagrams manifest that studied final states can be produced only with the interaction of the initial b quark and the gluon. Corresponding matrix elements for the signal process were obtained by using MadGraph 5.1.5.7 [19] where we implemented the KK gluon in MadGraph5 with FeynRules [20]. The signal events on the parton level were simulated by using the MadEvent package, a part of MadGraph. We simulated possible background processes,

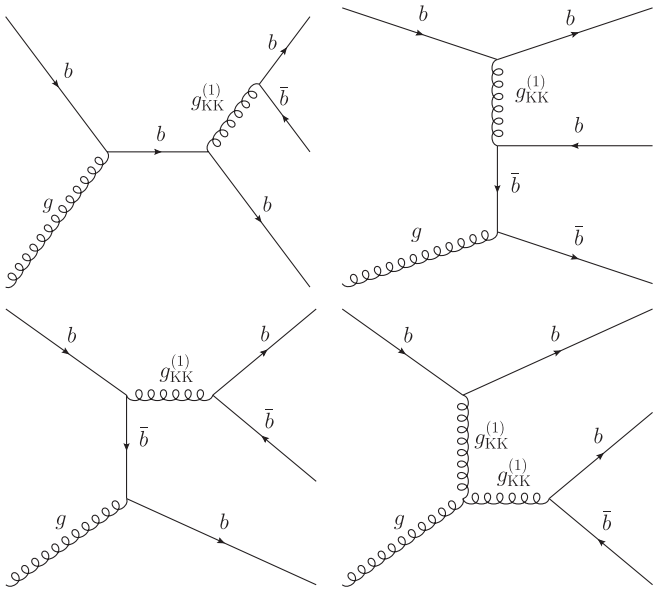

FIG. 1. The representative Feynman diagrams describing the studied processes with three b jets in the final state. The rest of the diagrams can be obtained by using one or more transformations from the following list: interchanging of b and $\bar{b}$ in a whole diagram, changing of order of initial partons, changing of order of final partons.

initial/final state radiations, hadronization and decays for both, the signal and background processes, by using Pythia 8.175 [21,22], the Monte-Carlo generator with leading-order expressions of matrix elements. All samples were generated for pp collisions at $\sqrt{s} = 14$ TeV by using the CTEQ6L1 parton distribution functions [23]. The factorization scale Q_F for the $2 \to 3$ processes was chosen to be equal to the geometric mean of the two smallest squared transverse masses of the three outgoing particles. The renormalization scale Q_R was chosen to be equal to the geometric mean of the squared transverse masses of the three outgoing particles. To save time in the simulations of the background $ab \to cde$ processes, the phase space cuts $\hat{p}_T(c) > 50$ GeV, $\hat{p}_T(d) > 50$ GeV, and $\hat{p}_T(e) > 50$ GeV on the transverse momentum of final particles in their center-of-mass system were applied.

For the simulation of the effects of a detector, we used Delphes 3.07 [24], a framework for a fast simulation of a generic collider experiment. The fast simulation of the detector includes a tracking system, a magnetic field of a solenoidal magnet affecting tracks of charged particles, calorimeters, and a muon system. The reconstructed kinematical values are smeared according to the settings of the detector simulation. For the jets reconstruction, Delphes uses the FastJet tool [25,26] with several implemented jet algorithms. In our simulations, we used the data file with standard settings for the ATLAS detector, provided by the tool. We used the k_T algorithm [27] with a cone radius parameter $R = 0.7$. The b-tagging efficiency is assumed to be 40%, independently on a transverse momentum and a pseudorapidity of a jet. A fake rate of the b-tagging algorithm is assumed to be 10% for c jets and 1% for light and gluon jets. These settings for the b tagging are standard for the ATLAS detector in the Delphes tool. No trigger inefficiencies are included in this analysis.

For the three-b-jets final states, it is difficult to select two b jets corresponding to the decay products of the KK gluon. In Fig. 2, the distribution of the invariant mass for all three b quark pairs for the signal process with $M_{g_{\mathrm{KK}}^{(1)}} = 1$ TeV and the scenario (2.11) is plotted. The resonance associated with a KK gluon is most evident in the invariant mass distribution of two jets with the highest transverse momenta in the invariant mass of two jets with the highest transverse momenta. Therefore, we assume this selection criterion: *Selection criterion 1:* The event must have exactly three b-tagged jets with the transverse momentum in the laboratory frame $p_T > 100$ GeV and the pseudorapidity $|\eta| < 2.5$. The invariant mass of two b jets b_1, b_2 with the highest transverse momenta must fulfill the condition $M_{b_1 b_2} > M^{\min}_{b_1 b_2}$ for a chosen $M^{\min}_{b_1 b_2}$.

Because of the b tagging and sufficiently high $M^{\min}_{b_1 b_2}$, the criterion effectively suppresses all QCD background processes (including a top quark production with all decay channels). In our analysis, the b tagging is used for jets

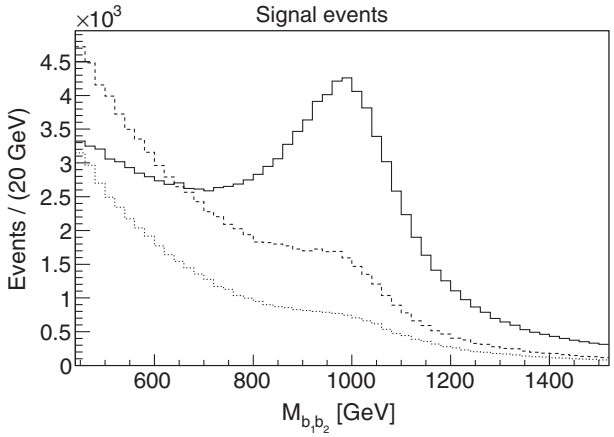

FIG. 2. The invariant mass distribution of all three b-quark pairs for the signal process for $M_{g_{\mathrm{KK}}^{(1)}} = 1$ TeV and the scenario (2.11). The full line corresponds to the pair with the two highest transverse momenta, the dashed line corresponds to the pair with the highest and lowest transverse momenta, and the dotted line corresponds to the pair with the lowest transverse momenta. The number of events in the histogram is scaled to the integrated luminosity of 10 fb^{-1} for pp collisions at $\sqrt{s} = 14$ TeV.

with very high transverse momentum (hundreds of GeV); see Fig. 3. At present, most of b-tagging algorithms are optimized and intensively tested for a lower range of jet transverse momenta. Therefore, we studied the possibility not to use the b tagging and to rely on strict selection cuts on the transverse momentum and invariant mass of the detected jets, instead: *Selection criterion 2*: The event must have at least three jets with the transverse momentum in the laboratory frame $p_T > 100$ GeV and

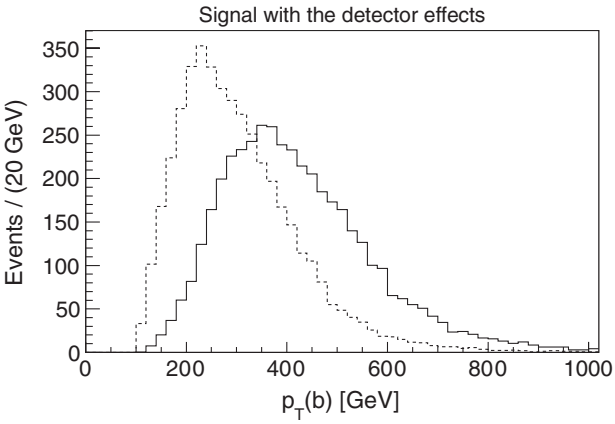

FIG. 3. The transverse momentum distribution for b jets selected in the scenario (2.11) with $M_{g_{\mathrm{KK}}^{(1)}} = 1$ TeV after applying selection criterion 1 and $M^{\min}_{b_1 b_2} = 450$ GeV for the signal events. The full line corresponds to the b jet with the highest transverse momentum, and the dashed line corresponds to the b jet with the second highest transverse momentum. The number of events in the histogram is scaled to the integrated luminosity of 10 fb^{-1} for pp collisions at $\sqrt{s} = 14$ TeV.

the pseudorapidity $|\eta| < 2.5$. The invariant mass of two jets b_1, b_2 with the highest transverse momenta must fulfill the condition $M_{b_1 b_2} > M^{\min}_{b_1 b_2}$ for a chosen $M^{\min}_{b_1 b_2}$.

We simulated the signal process for the four scenarios with the couplings (2.10), (2.11), (2.12), and (2.13) and for the masses of the KK gluon between 1 and 2.5 TeV. For the analysis, samples of 10^6 signal events were used. Assuming the integrated luminosity of 10 fb^{-1} per year (during a low luminosity LHC run), it corresponds to the data collected during the period with the length at least 2 years, depending on the $g^{(1)}_{\mathrm{KK}}$ mass and couplings. In Fig. 4, distributions of a $b_1 b_2$ invariant mass without and

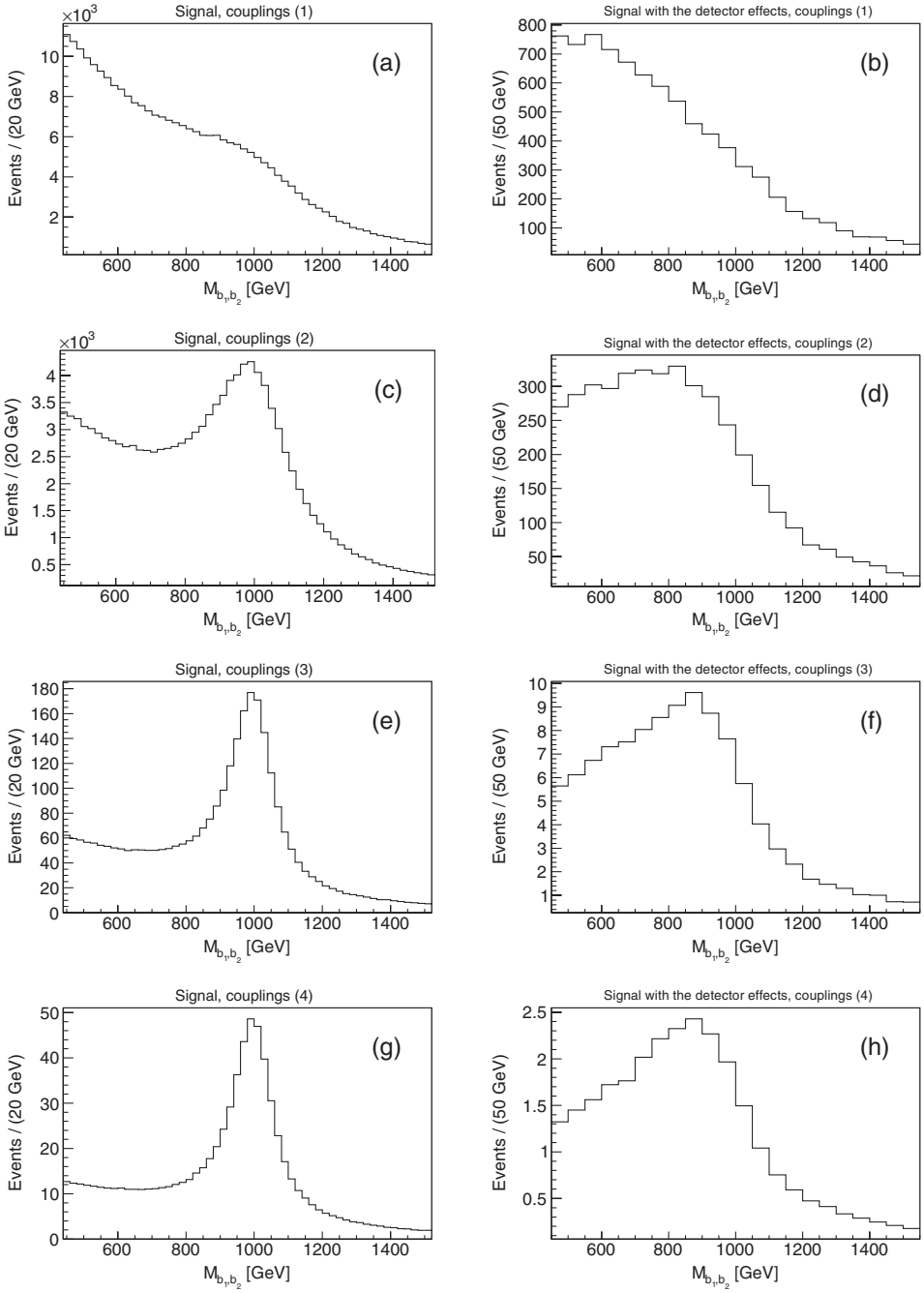

FIG. 4. The invariant mass distribution of the $b_1 b_2$ pairs of b jets with the highest transverse momenta for the signal process $pp \xrightarrow{g^{(1)}_{\mathrm{KK}}} 3b$ without [(a), (c), (e), and (g)] and with [(b), (d), (f), and (h)] the simulated effects of the ATLAS detector and selection criterion 1 (with $M^{\min}_{b_1 b_2} = 450$ GeV). $M_{g^{(1)}_{\mathrm{KK}}} = 1$ TeV was assumed and four scenarios with couplings (2.10), (2.11), (2.12), and (2.13) were studied [marked as (1)–(4), in the figure]. The number of events in the histogram is scaled to the integrated luminosity of 10 fb^{-1} for pp collisions at $\sqrt{s} = 14$ TeV.

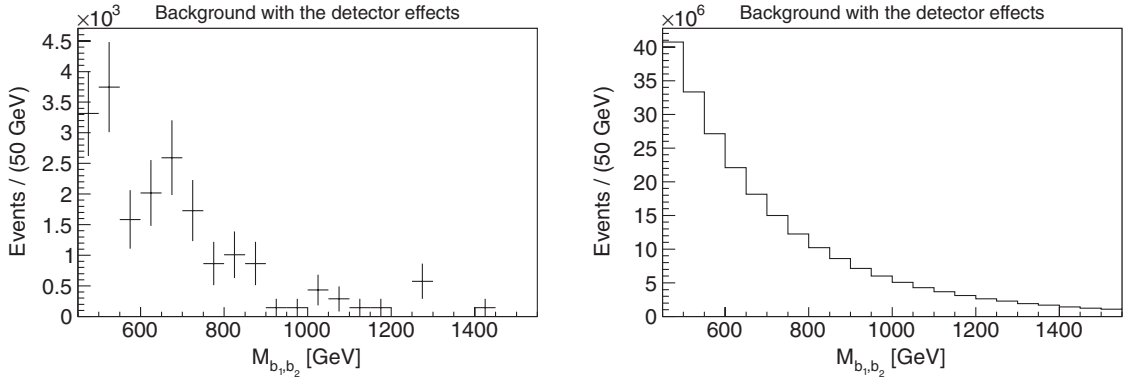

FIG. 5. The invariant mass distribution of the selected jet pairs for the background processes with the simulated effects of the ATLAS detector and selection criterion 1 on the left side and selection criterion 2 on the right side. $M^{\min}_{b_1 b_2}$ in both selection criteria was chosen to be 450 GeV. The number of events in the histogram is scaled to the integrated luminosity of 10 fb^{-1} for pp collisions at $\sqrt{s} = 14$ TeV.

with the simulated detector effects and selection criterion 1 for $M_{g^{(1)}_{\mathrm{KK}}} = 1$ TeV and couplings (2.10), (2.11), (2.12), and (2.13) are presented. All plots are scaled to the integrated luminosity of 10 fb^{-1}.

For the presented selection criteria, the most important background processes are the QCD production of three partons (quarks, antiquarks, and gluons). In the analysis, we used 100×10^6 simulated background events. Because of an extremely high cross section, it corresponds to the data collected only during 7×10^{-3} year (assuming the integrated luminosity of 10 fb^{-1} per year). In Fig. 5, the invariant mass distribution of the detected b jets (or objects supposed to be b jets) is plotted. On the left side, the events were selected by using selection criterion 1 (where the b tagging was used). Because of low statistics and rescaling the histogram, the error bars for each bin were plotted. The plot on the right side was performed by using selection criterion 2 (where the b tagging was not used). Applying the b tagging reduces background events dramatically; however, the low b-tagging efficiency can influence signal negatively, too: A number of observed signals are reduced.

As a signature of new physics, we use the number of selected events. For the integrated luminosity of 10 fb^{-1} and 100 fb^{-1}, we estimated the number of expected observed signal and background events (S and B) and the statistical significance $S/\sqrt{B}$. The significance of the deviation from the SM is proportional to the square root of the integrated luminosity. Therefore, it is easy to recompute the results for the higher integrated luminosity. We studied effects of variation of $M^{\min}_{b\bar{b}}$ on the statistical significance. In the presented results, we use the value of $M^{\min}_{b\bar{b}}$, for which the statistical significance $S/\sqrt{B}$ is maximal.

In Table I, we present the statistical significance $S/\sqrt{B}$ of our model for various values of $M_{g^{(1)}_{\mathrm{KK}}}$ and couplings. Selection criterion 1, with b tagging, was used for the

TABLE I. The statistical significance $S/\sqrt{B}$ of our model for various values of $M_{g^{(1)}_{\mathrm{KK}}}$ and couplings estimated for 10 fb^{-1} and 100 fb^{-1}. Selection criterion 1, using the b tagging, was used for the selection of the events. The presented errors correspond to the statistical errors related to our Monte Carlo simulations.

Scenario	$\frac{g^{(1)}_{\mathrm{light}}}{g_4}$	$\frac{g^{(1)}_{Q_3}}{g_4}$	$\frac{g^{(1)}_{b}}{g_4}$	$\frac{g^{(1)}_{t}}{g_4}$	$M_{g^{(1)}_{\mathrm{KK}}}$ [TeV]	$M^{\min}_{b_1 b_2}$ [GeV]	$S/\sqrt{B}$ for 10 fb^{-1}	$S/\sqrt{B}$ for 100 fb^{-1}
					1.0	550	62 ± 3	206 ± 10
					1.5	900	13 ± 2	43 ± 7
(2.10)	0	4	4	4	2.0	1300	4 ± 1	13 ± 3
					2.5	1450	1.5 ± 0.7	5 ± 2
(2.11)	0	1	4	4	1.0	720	36 ± 3	120 ± 10
					1.5	1300	8 ± 3	27 ± 10
					2.0	1450	2 ± 1	7 ± 3
					2.5	1450	0.7 ± 0.4	2 ± 1
(2.12)	0	1	1	4	1.0	730	1.04 ± 0.09	3.1 ± 0.3
(2.13)	0	1	0	4	1.0	750	0.26 ± 0.02	0.9 ± 0.07

TABLE II. The statistical significance $S/\sqrt{B}$ of our model for various values of $M_{g^{(1)}_{KK}}$ and couplings estimated for 10 fb^{-1} and 100 fb^{-1}. Selection criterion 2, without using the b tagging, was used for the selection of the events. The presented errors correspond to the statistical errors related to our Monte Carlo simulations.

Scenario	$\frac{g^{(1)}_{light}}{g_4}$	$\frac{g^{(1)}_{Q_3}}{g_4}$	$\frac{g^{(1)}_{b}}{g_4}$	$\frac{g^{(1)}_{t}}{g_4}$	$M_{g^{(1)}_{KK}}$ [TeV]	$M^{min}_{b_1 b_2}$ [GeV]	$S/\sqrt{B}$ for 10 fb^{-1}	$S/\sqrt{B}$ for 100 fb^{-1}
					1.0	500	9.23 ± 0.02	30.74 ± 0.07
(2.10)	0	4	4	4	1.2	550	4.323 ± 0.009	14.39 ± 0.03
					1.5	550	1.650 ± 0.003	5.45 ± 0.01
(2.11)	0	1	4	4	1.0	600	4.975 ± 0.009	16.57 ± 0.03
					1.2	750	2.203 ± 0.005	7.34 ± 0.02
					1.5	900	0.767 ± 0.002	2.554 ± 0.007
(2.12)	0	1	1	4	1.0	650	0.1339 ± 0.0002	0.4017 ± 0.0006
(2.13)	0	1	0	4	1.0	700	0.035 ± 0.001	0.117 ± 0.003

selection of the events. As expected, the deviation from the SM is strongly dependent on the coupling of a right-handed b quark to a KK gluon. For the first set of couplings (2.10), the effects of KK gluons could be observable with the significance at least 4σ for the mass of a KK gluon up to 2 TeV and the integrated luminosity of 10 fb^{-1} or for the mass of a KK gluon up to 2.5 TeV and the integrated luminosity of 100 fb^{-1}. For the second set of couplings (2.11), the effects of KK gluons could be observable with the significance of 8σ for the mass of a KK gluon up to 1.5 TeV and the integrated luminosity of 10 fb^{-1} or with the similar significance for the mass of a KK gluon up to 2 TeV and the integrated luminosity of 100 fb^{-1}. For the third set of couplings (2.12), the effects of KK gluons are observable only for the integrated luminosity of 100 fb^{-1} and $M_{g^{(1)}_{KK}} = 1$ TeV with the significance of 3σ. Because of the extremely low cross section of the signal process, for the fourth set of couplings (2.13) the effects of KK gluons are unobservable.

In Table II, we present analogous results for the simulations using selection criterion 2. Because of not applying the b tagging, a higher number of events are selected and hence the statistical errors of the obtained significance are smaller than ones of the results using selection criterion 1 as presented in Table I. For the couplings (2.10), the effects of KK gluons could be observable with the significance at least 4σ for the mass of a KK gluon up to 1.2 TeV and the integrated luminosity of 10 fb^{-1} or for the mass of a KK gluon up to 1.5 TeV and the integrated luminosity of 100 fb^{-1}. For the couplings (2.11), the effects of KK gluons could be observable with the significance at least 5σ for the mass of a KK gluon up to 1 TeV and the integrated luminosity of 10 fb^{-1} or for the mass of a KK gluon up to 1.2 TeV and the integrated luminosity of 100 fb^{-1}. Even for the integrated luminosity of 100 fb^{-1}, the effects of a KK gluon for the third set of couplings (2.12) are unobservable. The effects of a KK gluon for the fourth set of couplings (2.13) are unobservable like the result when selection criterion 1 is used.

IV. SUMMARY

We examined the possibility of observing the effects of the first excitation of a KK gluon at the LHC. We focused on the final states with three b jets. In our simulations, we studied pp interactions with the energy $\sqrt{s} = 14$ TeV. For the estimation of the detector effects, we supposed the ATLAS detector. We studied two kinds of selection criteria—with and without use of b tagging (selection criteria 1 and 2). We studied four sets of couplings (2.10), (2.11), (2.12), and (2.13) of a KK gluon to b and t quarks. As a signature of new physics, we used the number of selected signal (S) and background (B) events and the ratio $S/\sqrt{B}$, the statistical significance of the observed phenomenon. For selection criterion 1 and for the integrated luminosity of 100 fb^{-1}, the effects of a KK gluon will be observable with the significance at least 5σ for the scenario (2.10) with the KK gluon mass up to 2.5 TeV and for the scenario (2.11) with the KK gluon mass up to 2 TeV. Even for the integrated luminosity of 10 fb^{-1}, the effects of KK gluon will be observable with the significance at least 5σ for both the scenarios (2.10) and (2.11) for the KK gluon mass up to 1.5 TeV. The scenario (2.12) with a smaller coupling of a KK gluon to a right-handed b quark will be observable only for the high integrated luminosity of 100 fb^{-1} with the significance of 3σ. For the effects of a KK gluon for the scenario (2.13) with a vanishing coupling of a KK gluon to a right-handed b quark, the deviation from the SM will not be observable. As expected, the effects of a KK gluon will be observable with the higher significance for selection criterion 1. However, the signatures of a KK gluon will be evident even for the results applying selection criterion 2 not using the b tagging, though for lower KK gluon masses. For the integrated luminosity of 100 fb^{-1}, the effects of a KK gluon will be observable with the significance at least 5σ for the couplings (2.10) and (2.11) and the KK gluon mass up to 1.2 TeV.

If we compare our presented results for three b final states with ones for $b\bar{b}$ final states [14], we can conclude that the channel with three b jets are more sensitive to the effects of the KK gluon. It can be explained with a

tough selection requiring three b jets in the final state. It causes a sufficient suppression of the QCD background. On the other hand, the cross section of the signal process $pp \to 3b$ is roughly comparable to the cross section of $pp \to b\bar{b}$. Initial partons forming the final state with two b jets are both b quarks, whereas initial partons forming the final state with three b jets are one b quark and one gluon. The second configuration is more preferable since the distribution functions of a gluon enhances the cross section of $pp \to 3b$ integrating over the momentum.

ACKNOWLEDGMENTS

The work of M. A. is supported in part by Grants-in-Aid for Scientific Research from the Ministry of Education, Culture, Sports, Science and Technology (No. 25400280). The work of M. A. and K. S. is supported in part by the Research Program MSM6840770029 and by the project of International Cooperation ATLAS-CERN LG13009 of the Ministry of Education, Youth and Sports of the Czech Republic. The work of G. C. C is supported in part by Grants-in-Aid for Scientific Research from the Ministry of Education, Culture, Sports, Science and Technology (No. 24104502) and from the Japan Society for the Promotion of Science (No. 21244036). Numerical results published in this work were computed with the Supercluster of the Computing and Information Centre of the Czech Technical University in Prague.

[1] L. Randall and R. Sundrum, Phys. Rev. Lett. **83**, 3370 (1999); **83**, 4690 (1999).
[2] H. Davoudiasl, J. L. Hewett, and T. G. Rizzo, Phys. Lett. B **473**, 43 (2000).
[3] H. Davoudiasl, J. L. Hewett, and T. G. Rizzo, Phys. Rev. D **63**, 075004 (2001).
[4] S. Jung and J. D. Wells, J. High Energy Phys. 11 (2010) 001.
[5] K. Agashe, A. Delgado, M. J. May, and R. Sundrum, J. High Energy Phys. 08 (2003) 050.
[6] J. L. Hewett, F. J. Petriello, and T. G. Rizzo, J. High Energy Phys. 09 (2002) 030.
[7] M. Guchait, F. Mahmoudi, and K. Sridhar, J. High Energy Phys. 05 (2007) 103.
[8] B. Lillie, L. Randall, and L.-T. Wang, J. High Energy Phys. 09 (2007) 074.
[9] W.-F. Chang, J. N. Ng, and J. M. S. Wu, Phys. Rev. D **79**, 056007 (2009).
[10] M. Guchait, F. Mahmoudi, and K. Sridhar, Phys. Lett. B **666**, 347 (2008).
[11] CDF Collaboration, CDF Note No. 9164.
[12] CMS Collaboration, Report No. CMS PS TOP-11-009.
[13] ATLAS Collaboration, Report No. ATLAS-CONF-2012-029.
[14] M. Arai, G.-C. Cho, K. Smolek, and K. Yoneyama, Phys. Rev. D **87**, 016010 (2013).
[15] K. Agashe, A. Belyaev, T. Krupovnickas, G. Perez, and J. Virzi, Phys. Rev. D **77**, 015003 (2008).
[16] T. Gherghetta and A. Pomarol, Nucl. Phys. **B586**, 141 (2000).
[17] B. C. Allanach, F. Mahmoudi, J. P. Skittrall, and K. Sridhar, J. High Energy Phys. 03 (2010) 014.
[18] G.-C. Cho and Y. Kanehata, Phys. Lett. B **694**, 134 (2010).
[19] J. Alwall, M. Herquet, F. Maltoni, O. Mattelaer, and T. Stelzer, J. High Energy Phys. 06 (2011) 128.
[20] N. D. Christensen and C. Duhr, Comput. Phys. Commun. **180**, 1614 (2009).
[21] T. Sjöstrand, S. Mrenna, and P. Skands, J. High Energy Phys. 05 (2006) 026.
[22] T. Sjöstrand, S. Mrenna, and P. Skands, Comput. Phys. Commun. **178**, 852 (2008).
[23] J. Pumplin, D. R. Stump, J. Huston, H. L. Lai, P. M. Nadolsky, and W. K. Tung, J. High Energy Phys. 07 (2002) 012.
[24] S. Ovyn, X. Rouby, and V. Lemaitre, arXiv:0903.2225.
[25] M. Cacciari, G. P. Salam, and G. Soyez, Eur. Phys. J. C **72**, 1896 (2012).
[26] M. Cacciari and G. P. Salam, Phys. Lett. B **641**, 57 (2006).
[27] M. Cacciari, G. P. Salam, and G. Soyez, J. High Energy Phys. 04 (2008) 063.